

# Focal adhesion kinase – the reversible molecular mechanosensor

Samuel Bell and Eugene M. Terentjev

Cavendish Laboratory, University of Cambridge, Cambridge CB3 0HE, U.K.

## Abstract

Sensors are the first element of the pathways that control the response of cells to their environment. After chemical, the next most important cue is mechanical, and protein complexes that produce or enable a chemical signal in response to a mechanical stimulus are called mechanosensors. There is a sharp distinction between sensing an external force or pressure/tension applied to the cell, and sensing the mechanical stiffness of the environment. We call the first mechanosensitivity of the 1st kind, and the latter mechanosensitivity of the 2nd kind. There are two variants of protein complexes that act as mechanosensors of the 2nd kind: producing the one-off or a reversible action. The latent complex of TGF- $\beta$  is an example of the one-off action: on the release of active TGF- $\beta$  signal, the complex is discarded and needs to be replaced. In contrast, the focal adhesion kinase (FAK) in a complex with integrin is a reversible mechanosensor, which initiates the chemical signal in its active phosphorylated conformation, but can spontaneously return to its closed folded conformation. Here we study the physical mechanism of the reversible mechanosensor of the 2nd kind, using FAK as a practical example, and find how the rates of conformation changes depend on the substrate stiffness and the pulling force applied from the cell cytoskeleton. The results compare well with the phenotype observations of cells on different substrates.

Insert Received for publication Date and in final form Date.  
emt1000@cam.ac.uk

## 1 Introduction

Cells exist within a complex and varying environment. To function effectively, cells must collect information about their external environment, and then respond appropriately. Cell environment has a profound effect on cell migration and cell fate. It is also a major factor in metastasis of certain cancers (1, 2).

Sensing is the first part of the chain of events that constitute the cell response to external stimuli. Cells respond to a variety of cues; both chemical and mechanical stimuli must be transduced inside the cell. Mechanosensors are protein complexes that produce responses to mechanical inputs (3, 4). There are two distinct types of mechanosensing: reacting to an external force, or sensing the viscoelastic properties of the cell environment. We call the first mechanosensitivity of the 1st kind, and the latter mechanosensitivity of the 2nd kind.

Mechanosensitive ion channels (MSC), such as alame-thicin (5), are an example of mechanosensors of the first kind. MSCs exist in all cells and provide a non-specific response to stress in a bilayer membrane (6, 7). Local mechanical forces could be produced by many external factors, but MSC operation appears to be universal and quite simple. The ion channel is closed at low tension, opening as the tension exceeds a certain threshold, allowing ions to

cross the membrane. Traditionally, MSC operation is understood as a two-state model. There is a balance of energy gain on expanding the ‘hole’ under tension, and the energy penalty on increasing the hydrophobic region on the inner rim of the channel exposed to water on opening. These two-state systems (open/closed, or bonded/released) with the energy barrier between the states depending on applied force, are common in biophysics (8, 9). Rates of transition in these systems are often calculated using the ‘Bell formula’ (10), which has them increasing exponentially with the force. This is just the classical result of Kramers and Smoluchowski (11, 12), but it is invalid in the limit of high forces or weak barriers.

Mechanosensitivity of the 2nd kind is different in nature. The sensor has to actively measure the response coefficient (stiffness in this case, or matrix viscosity in the case of bacterial flagellar motion). On macroscopic scales (in engineering or rheometry) we can do this with two separate measurements: of force (stress) and of position (strain), or we could contrast two separate points of force application. One could also use inertial effects, such as impact or oscillation, to measure the stiffness or elastic constant of the element. None of these options are available on a molecular scale. The single sensor complex cannot measure relative displacements in the substrate, and the overdamped dynamics prevents any role of inertia. As a result, important biophysical work on focal

adhesion complexes (13) had to resort to an idea of dynamically growing force (or force-dependent velocity) applied to the proximal side of the two-spring sensor. Other important work (14) also relies on the dynamics of applied force with an elaborate construct of ‘catch-bonds’ whose stability increases with pulling force. In reality, the cell cytoskeletal filaments exert a pulling force that is constant on the time-scales involved. Further, the internal observable needed to sense stiffness in the catch-bond model (namely, fraction of unbound integrin-ECM bonds at a focal adhesion) does not have a clear downstream measurement process associated with it.

In an earlier study (15), we addressed the problem of how a mechanosensor of the 2nd kind should work, by developing a physical mechanism with a similar action to the two-spring model of Schwarz et al. (13, 16). That work focussed on the latent complex of TGF- $\beta$  (17–19), which is an irreversible one-off sensor: after the latent complex is ‘broken’ and active TGF- $\beta$  released, the whole construct has to be replaced. Here we apply these ideas to a reversible mechanosensor: protein tyrosine-kinase, now called focal adhesion kinase (FAK) (20–23). Phosphorylation of tyrosine residues of FAK is well known as the initial step of at least two signalling pathways of mechanosensing (24), leading to the cell increasing production of smooth muscle actin, and eventually fibrosis.

## 2 Biological system

As the name suggests, FAK is abundant in the regions of focal adhesions (21), which are developed in the cells on more stiff substrates, often also associated with fibrosis: the development of stress fibers of bundled actin filaments connecting to these focal adhesions and delivering a substantially higher pulling force. FAK is also present in cells of soft substrates in spite of the lack of any focal adhesions, and also in the lamellipodia during cell motility (22, 25, 26). There are several important players that we should also consider in this context: integrins, talin, paxillin, and the cytoskeleton. How do these components each contribute to the function of the complex?

The integrin family of transmembrane proteins link the extracellular matrix (ECM) to the intracellular actin cytoskeleton via a variety of protein-tyrosine kinases, one of which is FAK (27). Integrins are aggregated in focal adhesions, and they mediate the cell interaction with ECM (3). Activation of integrins is required for adhesion to the substrate; active integrins acquire ligand affinity and bind to the proteins of ECM (adhesion is obviously necessary for mechanosensing).

There is a large body of literature on integrins, with definitive reviews by Hynes (28, 29) explicitly stating that integrins are the mechanosensors. However, on close inspection, there turns out to be no evidence for that. Integrins

possess no catalytic activity of their own, and so cannot generate a signal (a good summary by Giancotti (30), while talking about ‘integrin signalling’, in fact, shows schemes where FAK is the nearest to cytoskeletal actin filaments). The important work by Guan et al. (31) establishes a clear correlation chain of extracellular fibronectin – transmembrane integrins – intracellular FAK, but it has no reason to assume that integrin is the sensing device on this chain.

There is a clear indication that phosphorylation of FAK is a key step in the mechanosensing process (4). However, the direct claim (31, 32) that the ECM-integrin link is the cause of FAK phosphorylation is not supported. Characteristically, a discussion by Schaller et al. (21) merely says that integrins ‘are there’ linking to the ECM, and that FAK phosphorylation is, in fact, the initial step of signalling: both statements are completely true, but one should not make a causal link that integrin is the reason for FAK phosphorylation. This important work (21) shows evidence that crosslinking integrins and ECM (i.e. making the ‘substrate’ stiffer) leads to an enhanced FAK phosphorylation, while conversely, a damage to integrin is connected with a reduced activation of FAK. It is also known that FAK would not activate without integrin binding to fibronectin ECM (31). Why is this?

In the native folded state of FAK, the FERM domain (the N-terminal of the protein) is physically bonded to the catalytic domain (kinase) (23, 33); we call this closed state, [c]. A conformational change occurs, which we shall call a transition to an open state, [o], when this physical bond is disrupted and the kinase separates from the FERM domain, see Fig. 1. Note that because there is a peptide chain link ([362–411] segment) between the FERM and kinase domains, they remain closely associated even after the conformational change – this is what makes FAK a reversible mechanosensor. The activation of the catalytic domain occurs in two steps: first the Tyr397 residue phosphorylates, which then allows binding of the Src kinase (34), which in turn promotes phosphorylation of several other sites of the catalytic domain (Tyr407, 576, 577, 861 and 925), making FAK fully activated. We shall call this state [a] in the subsequent discussion.

It is obvious that the large displacement required for the FAK conformational change cannot be achieved by purely chemical affinity: a mechanical work requires an energy input, which can only come from cytoskeletal forces (since no ATP hydrolysis occurs here). Recent work explicitly confirms that there is a critical role of tension, delivered from the actin cytoskeleton to FAK/integrin and involved in mechanosensing (35). A key role in this system is played by talin. There are many papers investigating the correlation of talin (and paxillin) with  $\beta$ -integrin and FAK, but recent advances clearly show that talin is capable of high stretching by a tensile force (36, 37), implying a function similar to that of titin in muscle cells (acting as an extension-limiter). It is also now clear that the immobile domain at the N-terminal of talin is associated with integrin, as well as the

FERM domain of FAK (36, 37), while the C-terminal of talin is associated with paxillin and the focal adhesion targeting (FAT) domain (C-terminal) of FAK. The actin filaments of the cytoskeleton exert a pulling force on this zone. Talin, therefore, acts as a scaffold for other proteins to arrange around, but more importantly, allows force to be transmitted from the cytoskeleton to the ECM, via integrin. All of these established facts are consistent with the model sketched in Fig. 1, where the integrin is the bridging element to the ECM, with the FERM domain localised near the cell membrane and N-terminal of talin. At the opposite end, the C-terminal of talin together with the FAT domain, can be pulled away by an applied force. This model is supported by the recent computational analysis (38) showing that the closed and the open states of FAK are reversibly reached by increasing and decreasing of pulling force.

The conformational change of FAK is the sensor in the act of signalling. There are many confusing and conflicting versions of events in the literature, for example, a common theme is that ‘FAK is phosphorylated in response to integrin engagement’ or ‘integrin receptors lead to FAK phosphorylation’. For us, it is clear that this is true only in the sense that integrin engagement allows the transmission of force through FAK. By connecting to the external environment, integrins facilitate the mechanosensing process, but their role extends no further than that. The work of Eck, Schaller et al. (23, 39), as well as more recent work of Guan et al. (40), have established the conformational change required for FAK phosphorylation – and although none of these authors made the link between this conformational change and the pulling force from the actin cytoskeleton (3); our sketch in Fig. 1, and the simulation study (38), make this point almost obvious. In the end, this is perhaps a semantic issue: one frequently finds a statement in the literature, that ‘FAK integrates inputs from a variety of cell surface-associated receptors’. Perhaps it is just a question of interpreting the word ‘input’ (41).

Let us explore the model that FAK sits inside the cell membrane, with its FERM domain either associated with the integrin-talin head assembly, or to the cell membrane in the vicinity of this assembly (35). Since we shall not consider the cell motility, one has to assume that FERM domain remains fixed with respect to the ECM reference. That is, if there is a deformation in (soft) ECM, then this point will move accordingly, with the integrin and the local cell membrane all joined together.

It is important to re-iterate a point: in order to achieve the large displacement associated with the [c]→[o] conformational transition of FAK, in the crowded intracellular environment, a mechanical work must be expended. This mechanical energy can only come from the active cytoskeletal forces, delivered via actin filaments. The link of FAK to the cytoskeleton via its FAT domain, combined with the fixing of the FERM domain near the integrin/membrane (35), allows force  $f$  generated by the cytoskeleton to be directly

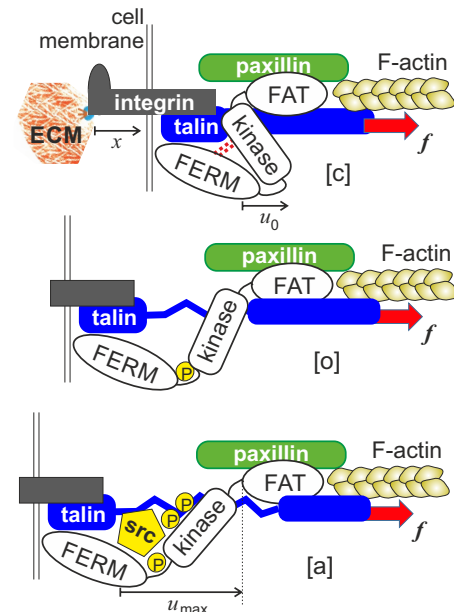


Figure 1: Schematic representation of FAK conformations. The FERM domain of FAK is associated with the integrin-talin head assembly, near the cell membrane, while the FAT domain is associated with paxillin as well as the rod domain (C-terminal) of talin, which contains the actin binding site (35). On applying the pulling force, talin extends its middle section, allowing the force transmission to FERM-kinase physical bond. In the closed state [c] the kinase domain is inactive and the whole FAK protein is in its native low-energy state. Once the physical bond holding the FERM domain and the kinase together is broken, the protein adopts the open conformation [o]. In the open state, first the Tyr397 site spontaneously phosphorylates, which in turn allows binding of Src and further phosphorylation of the kinase – turning it into the active state [a], see (33, 39, 40).

transmitted through the FERM-kinase structure. This, we believe, is the simplest way to account for mechanical work performed on the FERM-kinase structure.

We can now record these conformational changes in the FAK structure in the schematic plot of the ‘unfolding free energy’, which will play the role of potential energy  $U(u)$  for the subsequent stochastic analysis of the sensor action, illustrated in Fig. 2. The concept of such unfolding free energy is becoming quite common (42), when one identifies an appropriate reaction coordinate and discovers that a deep free energy minimum exists in the native folded state, with a broad range of intermediate conformations having a ragged, but essentially flat free energy profile – before the final full unfolding rises the energy rapidly. Figure 2(a) needs to be looked at together with the conformation sketches in Fig. 1: the native state [c] needs a substantial free energy ( $\Delta G_o$ ) to disrupt the physical bonds holding the kinase and FERM

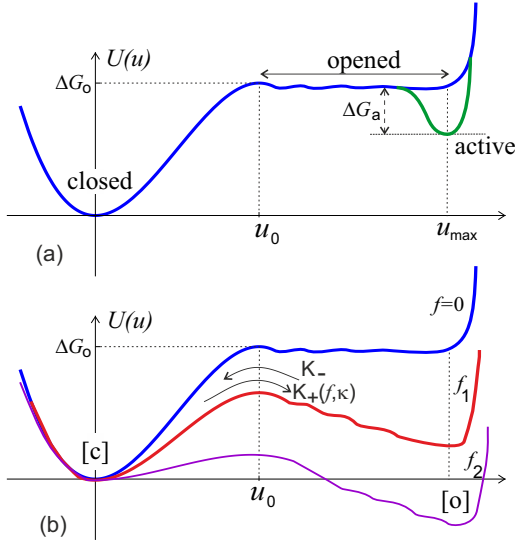


Figure 2: Schematic potential energy of different FAK conformations. (a) The force-free molecule has its native folded state [c], compare with Fig. 1. The binding free energy  $\Delta G_o$  has to be overcome to separate the kinase from the FERM domain, after which there is a range of conformations of roughly the same energy is achieved by further separating these two domains in the open state [o]. At full separation (distance  $u_{\max}$ ) the Src binding and kinase phosphorylation lead to the active state [a] of the protein, with the free energy gain  $\Delta G_a$ . (b) When a pulling force is applied to this system ( $f_2 > f_1 > 0$ ) the potential energy profile distorts, so that both [o] and [a] states shift down in energy by the same amount of  $-f \cdot u_{\max}$ .

domains together. However, once this is achieved, there are only very minor free energy changes due to the small bending of the [362-411] segment (23), when the kinase and FERM domains are gradually pulled apart. This change is measured by the relative distance, which we label  $u$  in the sketch and the plot. If one insists on further separation of the protein ends, past the fully open conformation [o] at  $u = u_{\max}$ , the protein will have to unfold at a great cost to the free energy. Binding of Src and phosphorylation (i.e. converting the [o] state into the [a]) lowers the free energy of the fully open conformation by an amount  $\Delta G_a$ . Note that there is no path back to the closed state, once the kinase is activated: one can only achieve ‘autoinhibition’ (23) via the [a]→[o]→[c] sequence.

If we accept the basic form of the protein potential profile, as shown in Fig. 2(a), the effect of the pulling force  $f$  applied to FAK from the actin cytoskeletal filaments is reflected by the mechanical work:  $U(u) - f \cdot u$ . If we take the reference point  $u = 0$  as the closed native conformation, then the opening barrier reduces by:  $\Delta G_o - f \cdot u_0$ . Similarly, the free energy of the fully open state [o] becomes lower by:  $\Delta G_o - f \cdot u_{\max}$ , see Fig. 2(b). Since the binding free energy

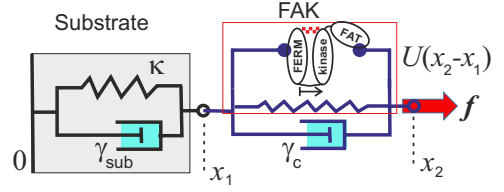


Figure 3: A scheme of the 2-spring model used to produce equations (1). The viscoelastic substrate is characterised by its elastic stiffness and stress-relaxation time given by  $\gamma_{\text{sub}}/\kappa$ . The conformational change of FAK is described by a potential  $U(u)$ , see Fig. 2, and the associated relaxation time determined by the damping constant  $\gamma_c$ .

of Src and phosphorylation does not depend on the applied force, the energy level of the active state [a] lowers by the same amount of  $\Delta G_a$  relative to the current [o] state.

### 3 Stochastic two-spring model

The two-spring model discussed in detail by Schwarz et al. (13, 16) and reproduced many times afterwards (24) is a correct concept, except that it needs to take into account that both the viscoelastic substrate and the sensor, described by the potential energy  $U(u)$ , experience independent thermal excitations. This is inevitable at the molecular level, since we are considering the mechanical damping in the substrate (as we must) and in the sensor (as we will). In the overdamped limit all forces must balance along the series of elements, and only thermal fluctuations – independent in the two elements – can create a relative displacement in the middle of this series (i.e. on the sensor). It is this relative displacement that one needs to ‘measure’ the stiffness.

Following the logic outlined in greater detail in earlier work (15), we introduce two independent stochastic variables. The first is  $x_1 = x$ , which measures the displacement of the substrate with respect to its undeformed reference state, and therefore also marks the position of the FERM domain (or the origin of the length  $u$ ). The second is  $x_2$  that measures the displacement of the far end of the kinase domain: the point of application of the pulling force  $f$ , see Fig. 3 for an illustration. These two variables satisfy a pair of coupled overdamped Langevin equations:

$$\begin{aligned} \gamma_{\text{sub}} \dot{x}_1 &= -\kappa x_1 + \frac{dU}{d(x_2 - x_1)} + \sqrt{2k_B T \gamma_{\text{sub}}} \cdot \zeta(t), \\ \gamma_c \dot{x}_2 &= -\frac{dU}{d(x_2 - x_1)} + f + \sqrt{2k_B T \gamma_c} \cdot \zeta(t), \end{aligned} \quad (1)$$

where  $\kappa$  is the elastic stiffness and  $\gamma_{\text{sub}}$  the damping constant of viscoelastic substrate, while  $\gamma_c$  is the (completely independent) damping constant for the conformational changes in FAK structure; the base stochastic process  $\zeta(t)$  is assumed to be Gaussian and normalised to unity. Note that it is the

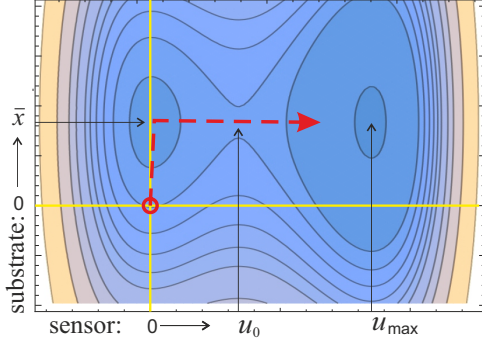


Figure 4: The 2D contour plot of the effective potential  $V_{\text{eff}}(x, u)$  at a certain value of pulling force applied. The position of substrate anchoring has moved from  $x = 0$  to  $\bar{x} = f/\kappa$ , and the depth of the energy well of the [o] state has lowered to  $\Delta G_o - fu_{\text{max}}$ . The dashed line shows the trajectory of the system evolution that leads to the opening of the [c] state.

difference in independent position coordinates  $u = x_2 - x_1$ , that affects the sensor potential  $U(u)$ . The problem naturally reduces to a 2-dimensional Smoluchowski equation for the variables  $x = x_1(t)$  for the substrate, and  $u(t)$  for the FAK conformations, with the corresponding diffusion constants  $D_i = k_B T / \gamma_i$ , and the Cartesian components of diffusion current:

$$J_i = -\frac{k_B T}{\gamma_i} e^{-V_{\text{eff}}/k_B T} \nabla_i \left( e^{V_{\text{eff}}/k_B T} P \right), \quad (2)$$

where  $P(x, u; t)$  is the probability distribution of the process, and

$$\begin{aligned} V_{\text{eff}}(x_1, x_2) &= \frac{1}{2} \kappa x_1^2 - f x_2 + U(x_2 - x_1) \\ &= \frac{1}{2} \kappa x^2 - f x + U(u) - f u \end{aligned} \quad (3)$$

represents the effective potential landscape over which the substrate and the mechanosensor complex move, subject to thermal excitation and the external constant force  $f$ .

The effective Kramers problem of escape over the barrier has been solved many times over the years (8, 11, 12, 43, 44). The multi-dimensional Kramers escape problem, with the potential profile not dissimilar to that in Fig. 4 was also solved many times (45, 46). Unlike many previous approaches, we will not allow unphysical solutions by mistreating the case of very low/vanishing barrier. In the case when the effective potential barrier is not high enough to permit the classical Kramers approach of steepest descent integrals, one of several good general methods is via Laplace transformation of the Smoluchowski equation (12, 47). The compact answer for the mean time of first passage from the closed state [c] to the top of the barrier of height  $Q$  a distance

$\Delta u$  away is:

$$\tau_+ = \frac{\Delta u^2}{D} \left[ \left( \frac{k_B T}{Q} \right)^2 \left( e^{Q/k_B T} - 1 \right) - \frac{k_B T}{Q} \right]. \quad (4)$$

This is a key expression, which gives the standard Kramers thermal-activation law when the barrier is high (which is also the regime when the ‘Bell formula’ is valid), but in the limit of low barrier it correctly reduces to the simple diffusion time across the distance  $\Delta u$ .

#### 4 Rate of [c]-[o] transition: $K_+$

There are many complexities regarding choosing an optimal path across the potential landscape  $V_{\text{eff}}(x, u)$ , some of which are discussed in (45, 46), but we are aiming for the quickest way to a qualitatively meaningful answer. As such, we shall assume that the reaction path consists of two ‘legs’: from the origin down to the minimum of the potential, which is shifted to  $\bar{x} = f/\kappa$  due to the substrate deformation, and from this minimum over the saddle (barrier) into the open state of FAK conformation. The average time along the first leg is given by the equation (4) with the distance  $\Delta u = \bar{x}$  and the negative energy level  $E = -f^2/2\kappa$ , with the diffusion constant determined by the damping constant of the substrate:

$$\tau_{\text{sub}} = \frac{2\gamma_{\text{sub}}}{\kappa} + \frac{4\gamma_{\text{sub}} k_B T}{f^2} \left( e^{-f^2/2\kappa k_B T} - 1 \right). \quad (5)$$

Here the ratio  $\gamma_{\text{sub}}/\kappa$  is the characteristic stress-relaxation time of the viscoelastic substrate (48), which will play a significant role in our results. Naturally,  $\tau_{\text{sub}} = 0$  when there is no pulling force and the minimum is at  $(0, 0)$ .

In the region between the minimum of  $V_{\text{eff}}$  and the potential barrier, a number of earlier papers (15, 44, 46) have used the effective cubic potential to model this portion of  $U(u)$ . In this case, when the pulling force is applied, the barrier height is reducing as:  $E = \Delta G_o (1 - 2fu_0/3\Delta G_o)^{3/2}$ , while the distance between the minimum [c] and the maximum at the top of the barrier is reducing as:  $\Delta u = u_0 (1 - 2fu_0/3\Delta G_o)^{1/2}$ . Substituting these values into equation (4), we find the mean passage time over the barrier:

$$\begin{aligned} \tau_{\text{esc}} &= -\frac{\gamma_c u_0^2}{\Delta G_o \left( 1 - \frac{2fu_0}{3\Delta G_o} \right)^{1/2}} \\ &+ \frac{\gamma_c k_B T u_0^2}{\Delta G_o^2 \left( 1 - \frac{2fu_0}{3\Delta G_o} \right)^2} \left( e^{\Delta G_o (1 - \frac{2fu_0}{3\Delta G_o})^{3/2} / k_B T} - 1 \right). \end{aligned} \quad (6)$$

In the limit of high barrier  $\Delta G_o \gg k_B T$  and small force this expression becomes proportional to  $e^{-(\Delta G_o - Fu_0)/k_B T}$ , i.e. recovers the Bell formula that people use widely. When the force increases towards the limit  $F_c = 3\Delta G_o/2u_0$ , this time

$\tau_{\text{esc}}$  reduces to zero: there is no more barrier left to overcome, and the minimum of  $V_{\text{eff}}$  shifts to coincide with the entrance to the [o] state.

The overall rate constant of ‘escape’  $K_+$  (the transition [c]→[o]) is then determined as the inverse of the total time:  $K_+ = (\tau_{\text{sub}} + \tau_{\text{esc}})^{-1}$ . From examining equations (5) and (6) it is evident that the rate of FAK opening is a strong function of the pulling force  $f$ , but more importantly: it changes dramatically with the substrate stiffness  $\kappa$ . The important exponential factor  $e^{f^2/2\kappa k_B T}$  appears in  $\tau_{\text{sub}}$ ; it was discussed at length in (15) where it has emerged in a very different approach to solving a similar problem, and interpreted as an effective ‘enzyme effect’ of the system being confined at the bottom of the potential well before jumping over the barrier.

In order to analyse and plot it, we need to scale the rate constant  $K_+$  to convert it into non-dimensional values. First, we can identify a characteristic time scale of the FAK conformational change:  $u_0^2 \gamma_c / \Delta G_o$ . The two control parameters defining the opening rate  $K_+$  are also made non-dimensional, scaling the force by the natural value of the FERM-kinase holding potential,  $\Delta G_o / u_0$ , and scaling the substrate stiffness by  $\Delta G_o / u_0^2$ . After these transformations, and some algebra, we obtain:

$$K_+ = \left( \frac{\Delta G_o}{u_0^2 \gamma_c} \right) \frac{g \bar{f}^2 (1 - 2\bar{f}/3)^2 \zeta}{4 (1 - 2\bar{f}/3)^2 \Psi_1[f] + \bar{f}^2 \zeta \Psi_2[f]}, \quad (7)$$

with shorthand notations

$$\Psi_1[f] = \exp[-g \bar{f}^2 / 2\bar{\kappa}] + g \bar{f}^2 / 2\bar{\kappa} - 1,$$

$$\Psi_2[f] = \exp[g (1 - 2\bar{f}/3)^{3/2}] - g (1 - 2\bar{f}/3)^{3/2} - 1,$$

where the non-dimensional abbreviations stand for: the energy barrier  $g = \Delta G_o / k_B T$ , the force  $f = \bar{f} \cdot \Delta G_o / u_0$ , the substrate stiffness  $\kappa = \bar{\kappa} \cdot \Delta G_o / u_0^2$ , and the ratio of damping constants  $\zeta = \gamma_c / \gamma_{\text{sub}}$ . There are several key effects predicted by this expression for the rate of FAK opening under force, while attached to a viscoelastic base, which we can examine by plotting it. However, we must know or estimate the values of many material parameters that determine its entries.

#### Estimates of material parameters

The effectiveness of FAK as a mechanosensor of the 1st kind, i.e. responding to an increase of applied force with a conformation change, is illustrated in Fig. 5. In order to make plots with parameter values corresponding to a real cell, let us start with the strength of physical bond holding the FERM and kinase domain in the closed (autoinhibited) state:  $\Delta G_o / k_B T \approx 25$ , which is  $\approx 15$  kcal/mol at room temperature. This value is reasonable for the internal physical (hydrophobic) bonding between domains of a complex protein, and it is also the estimate for FAK opening barrier

obtained in MD simulation study (38). We can also take the position of the barrier from the same study:  $u_0 = 0.9$  nm, again, a reasonable value for the protein domain structure. This makes the critical force  $F_c = 3\Delta G_o / 2u_0 \approx 110$  pN. This is a high force that is likely to unfold most proteins, and is also unlikely to be generated by a single actin filament of a cell cytoskeleton. For comparison, the force to fully unfold integrin is quoted as 165 pN (49). Buscemi et al. (49) also quoted 40 pN as the force required to unlock the physical bond of the latent complex of TGF- $\beta$ 1. Other reports investigate the force required to disrupt the fibronectin-integrin-cytoskeleton linkage, finding the value of 1-2 pN (50, 51). For a force  $f = 10$  pN, the scaled non-dimensional value  $\bar{f} \approx 0.1$ .

We also need to estimate typical values of substrate stiffness. If a half-space occupied by an elastic medium (e.g. gel substrate or glass plate) with the Young modulus  $Y$ , and a point force  $F$  is applied along the surface (modelling the pulling of the integrin-ECM junction, Fig. 1), the response coefficient (spring constant) that we have called the stiffness is given by  $\kappa = (4/3)\pi Y \xi$ , where  $\xi$  is a short-distance cutoff: essentially the mesh size of the substrate. This is a classical relation going as far back as Lord Kelvin (52). For a weak gel with  $Y = 10$  kPa, and a characteristic network mesh size  $\xi = 10$  nm, we obtain  $\kappa = 4.2 \cdot 10^{-4}$  N/m, and the scaled non-dimensional parameter  $\bar{\kappa} \approx 0.003$ . On a stiff mineral glass with  $Y = 10$  GPa, we must take the characteristic size to be a ‘cage’ size (slightly above the size of a monomer),  $\xi = 1$  nm, which gives  $\kappa = 42$  N/m, and the non-dimensional parameter  $\bar{\kappa} \approx 300$ . A typical stiff plastic has a value about 10 times smaller. So a large spectrum of values  $\bar{\kappa}$  could be explored by living cells.

Finally, we need estimates of the damping constants. The simulation study (38) determined a value for the diffusion constant of the FAK complex:  $D = k_B T / \gamma_c \approx 6 \cdot 10^{-12} \text{ m}^2 \text{ s}^{-1}$ . At room temperature, this gives a value for the damping constant:  $\gamma_c = 7 \cdot 10^{-10} \text{ kg s}^{-1}$ . Then, the overall scale of the rate  $K_+$  is  $\Delta G_o / u_0^2 \gamma_c \approx 7 \cdot 10^6 \text{ s}^{-1}$  (see equation (7)).

To estimate the damping constant of the viscoelastic substrate, we assessed the characteristic time of its stress relaxation, which is the ratio  $\gamma_{\text{sub}} / \kappa$  in our parameter notation. The order of magnitude of stress relaxation time in gels is quite long, up to 100 s. Using the values of  $\kappa$  for gels given above, the typical damping constant is calculated as:  $\gamma_{\text{sub}} \approx 0.04 \text{ kg s}^{-1}$ , and the ratio  $\zeta = \gamma_c / \gamma_{\text{sub}} \sim 7 \cdot 10^{-8}$ . For stiff substrates, we need the vibration damping time in a solid glass (one must not confuse this with the creep stress relaxation, extensively studied in glasses (53) but not related to our viscoelastic response). The characteristic time we are looking for is closer to the  $\beta$ -relaxation time of the ‘cage’ motion (54), and the literature gives values in the range of 0.01 s (55). Combining the corresponding value of stiffness  $\kappa$  discussed above gives the damping constant



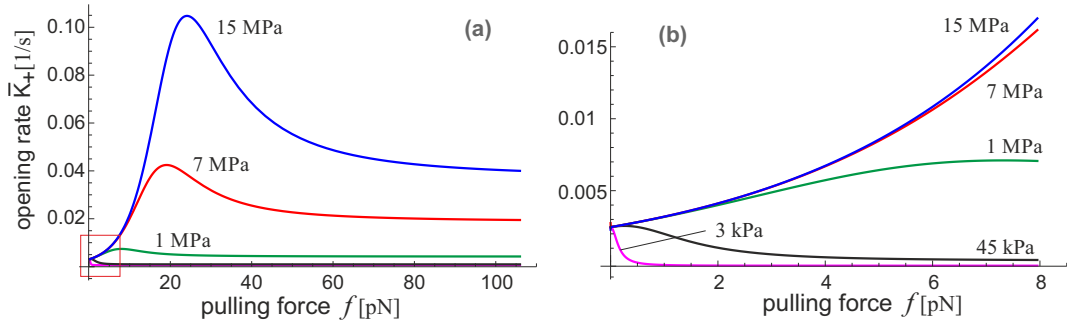


Figure 5: The rate constant of FAK opening  $K_+(f, \kappa)$  is plotted as a function of the pulling force  $f$ , for several values of given substrate stiffness labelled on the plot. Here we take the bond strength of the FERM-kinase link  $\Delta G_o = 25k_B T$ ,  $u_0 = 0.9$  nm, and the ratio of damping constants  $\gamma_c/\gamma_{\text{sub}} = 10^{-8}$  (see the discussion in text about the representative values of parameters). The plot (a) illustrates the overall nature of this response, while the plot (b) zooms in the region of small forces which are biologically relevant.

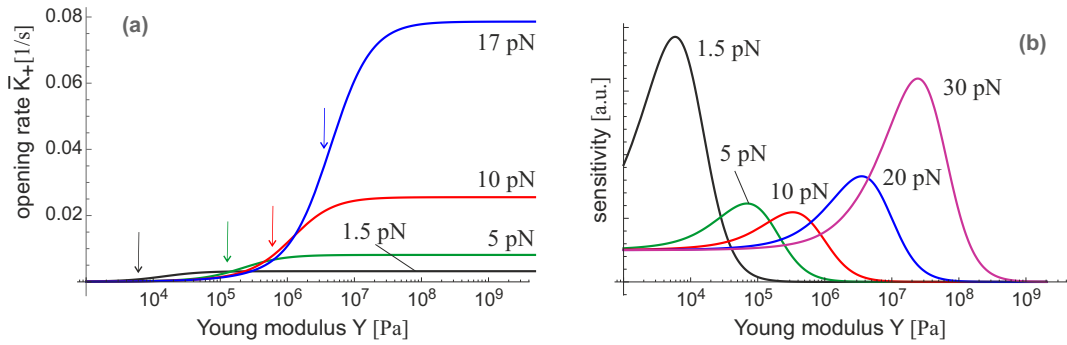


Figure 6: (a) The rate constant of the  $[c] \rightarrow [o]$  transition  $K_+(f, \kappa)$  plotted against the substrate stiffness (on logarithmic scale), for several values of the pulling force  $f$  (focusing on the biologically relevant low-force region). As in Fig. 5, we take  $\gamma_c/\gamma_{\text{sub}} = 10^{-8}$  for illustration. The arrows point at the inflection point on each curve, i.e. the region of maximum sensitivity. (b) The plot of ‘sensitivity’  $dK_+/d\kappa$  for the same parameters, illustrating the maximum sensitivity range at each level of pulling force.

$\gamma_{\text{sub}} \approx 0.4 \text{ kg s}^{-1}$ , and the ratio  $\zeta = \gamma_c/\gamma_{\text{sub}} \sim 10^{-9}$  or less.

Having established realistic parameter values, we can plot the behaviour of our model. Figure 5(a) highlights the rapid increase in the rate that FAK opens (and its subsequent phosphorylation) on stiffer substrates. The cell remodels itself in response to FAK activation, increasing the pulling force. This increases the level of FAK activation until a maximum rate is reached. Any increase in force beyond this point decreases the rate of FAK opening. This would act as a mechanism for negative feedback, which settles the cell tension in homeostasis. The stiffer the substrate, the higher the rate of FAK activation and, accordingly, the more  $\alpha$ -SMA stress fibers one would find in this adjusted cell (leading to morphological changes such as fibroblast-myofibroblast transition, or the fibrosis of smooth muscle cells). The plot 5(b) zooms in to the region of small forces and highlights the effect of soft substrates. On substrates with sufficiently small

$\kappa$  there is no positive force that gives a maximum in the opening rate. Thus, any pulling force on the FAK-integrin-ECM chain has the effect of lowering the activation of FAK relative to the untensioned state, and so the cell does not develop any great tension in the cytoskeleton. This is consistent with the observation that cells do not develop focal adhesions on soft gels.

Figure 6 presents the same rate of FAK opening, but focuses on the effect of substrate stiffness. As we have shown, the possible range of parameter  $\kappa$  is large, and so we plot the axis of stiffness in logarithmic units. The rate of FAK activation has a characteristic (generic) form of any sensor in that it undergoes a change between the ‘off’ and ‘on’ states. The latter is a state of high rate of FAK opening and the subsequent phosphorylation, initiating the signalling chains leading to more actin production and increase of stress fibers. For each cell, characterised by a specific level of pulling force, the substrate could be ‘too soft’, meaning that FAK does not activate at all – and also ‘too stiff’, where the

rate of activation reaches a plateau and no longer responds to further stiffening. Between these two limits, there is a range of maximum sensitivity where the rate of activation directly reflects the change of substrate stiffness. Figure 6(b) highlights this by presenting the ‘sensitivity’ directly as the value of the derivative  $dK_+/d\kappa$ . We see that cells with a higher pulling force (i.e. with high actin-myosin activity and developed stress fibers) are sensitive to the substrates in the stiff range. In contrast, cells that exert a low pulling force (i.e. no stress fibers, low actin-myosin activity) are mostly sensitive to soft substrates. This is in good agreement with broad observations about the cell mechanosensitivity of the 2nd kind, and their response to substrate stiffness.

## 5 Substrate stress relaxation regulates $K_+$

There are many indications in the literature that not only the substrate stiffness, but also the degree of viscoelasticity (often measured by the characteristic time of stress relaxation) have an effect on cell mechanosensitivity (48). It is actually irrelevant what particular viscoelastic model one should use for the substrate, and certainly impossible to have a universal model covering the highly diverse viscoelasticities of gels, filament networks, and disordered solids like plastic and glass. In the spirit of our ultimately simplified viscoelastic model expressed in equations (1), the single parameter characterising viscoelasticity could be the characteristic time scale  $\gamma_{\text{sub}}/\kappa$ : this could be a measure of the actual stress relaxation time of different substrates. This would be a very short timescale in stiff solids, while complex disordered filament networks like a typical ECM would have this time measured in minutes or hours. We now find that the rate of FAK opening is strongly affected by the viscoelastic relaxation properties of the substrate.

We assume that the damping constant  $\gamma_c$  of the FAK complex remains the same. In that case, Fig. 7 shows how changing the damping constant of the substrate  $\gamma_{\text{sub}}$  (or the associated loss modulus of the viscoelastic material) can regulate the FAK mechanosensor. All curves retain exactly the same topology and amplitude, but the range of sensitivity shifts in either direction. The green curve for  $\zeta = \gamma_c/\gamma_{\text{sub}} = 10^{-8}$  is the same as the green curve for  $f = 5$  pN in both plots in Fig. 6. We find that for substrates with greater stress relaxation (i.e. greater loss modulus, or  $\gamma_{\text{sub}}$ , leading to the ratio  $\zeta$  becoming smaller), the FAK sensor will activate at higher stiffnesses. In other words, in stiffer substrates, stress relaxation suppresses the response of a sensor with respect to a strictly elastic substrate.

We also see the strong effect of substrate viscoelasticity on the absolute value of rate of FAK activation  $K_+$ . Figure 8 shows a comparison of the effect between two realistic substrates: a stiff rubber/plastic with the Young modulus of  $\sim 25$  MPa (yet not a completely rigid glass) and a soft rubber with the Young modulus  $\sim 0.2$  MPa (yet not a very soft

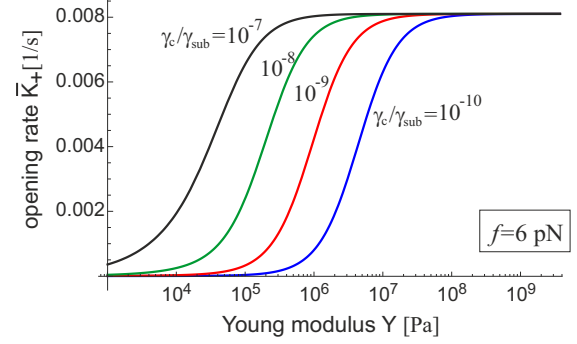


Figure 7: The rate of the  $[c] \rightarrow [o]$  transition  $K_+(f, \kappa)$  plotted against the substrate stiffness for a fixed (low) value of pulling force and a set of changing stress-relaxation properties of the substrate measured by the ratio  $\gamma_c/\gamma_{\text{sub}}$ , cf. equations (1) and (7). The range of maximum sensitivity shifts to the effectively stiffer substrate range for materials with higher damping constant  $\gamma_{\text{sub}}$ .

gel). The same range of change of  $\gamma_{\text{sub}}$  is tested, and here we see how the material with the same elastic modulus but a higher loss factor (i.e. lower ratio  $\zeta$ ) effectively produces a response similar to a softer substrate. This might appear counter to the conclusion one draws from Fig. 7 (where the range of sensitivity shifted to stiffer substrate), but one must remember that we are exploring different aspects of the same expression  $K_+(f, \kappa)$ : the information conveyed by Fig. 5 is exactly the same as that in Fig. 6(a).

## 6 Rate of [o]→[c] transition: $K_-$

The free energy profile of the conformation change leading to the  $[o] \rightarrow [c]$  transition (i.e. the spontaneous return of FAK to its native folded conformation: the autoinhibition) is essentially described by the linear potential, see Fig. 2. From the reference point of  $[o]$  state, the energy barrier is  $E = f(u_{\text{max}} - u_0)$ , and we should assume that the physical distance the FERM domain needs to travel remains constant: it is determined by the extent of the protein structure (23, 39). This process also does not depend on the substrate stiffness. As a result, the rate of the folding transition is the inverse of the mean first-passage time (4) with these parameters:

$$K_-(f) = \frac{f}{\gamma_c \Delta u} \left( \frac{k_B T}{f \Delta u} \left[ e^{f \Delta u / k_B T} - 1 \right] - 1 \right)^{-1}, \quad (8)$$

with the shorthand notation  $\Delta u = (u_{\text{max}} - u_0)$ . When the force is high, and the  $[o]$  state has a deep free-energy minimum generated by this external mechanical work, see Fig. 2(b), this rate reduces exponentially with pulling force:  $K_- \approx (f^2 / \gamma_c k_B T) e^{-f \Delta u / k_B T}$ . This reflects the increasing stability of the  $[o]$  state when FAK is pulled with a high force, even before it phosphorylates and further stabilises in the active state  $[a]$ . On the other hand, at vanishing force:



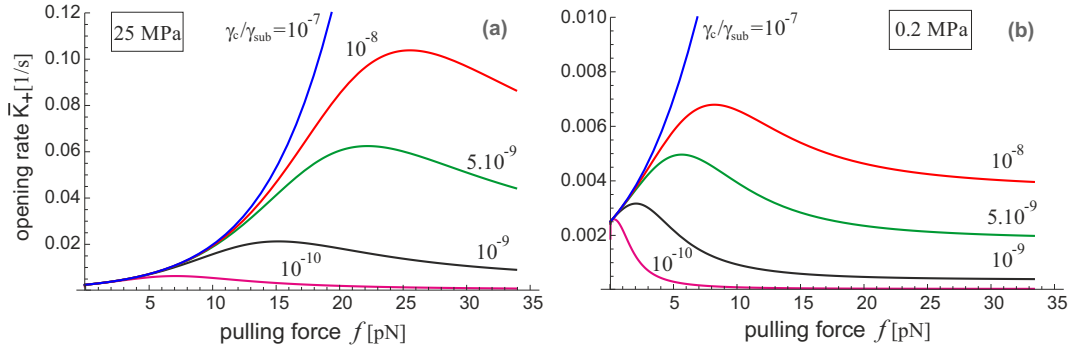


Figure 8: The rate of the  $[c] \rightarrow [o]$  transition  $K_+(f, \kappa)$  plotted against the pulling force  $f$  (in the biologically relevant range of small forces) for a set of values  $\gamma_c/\gamma_{\text{sub}}$  labelled on the plots representing the change in stress-relaxation characteristics of the substrate. Plot (a) represents stiffer substrates (Young modulus  $Y \approx 25$  MPa), and plot (b) – softer substrate ( $Y \approx 0.2$  MPa).

$f \rightarrow 0$ , this rate becomes  $K_- \approx 2k_B T / \gamma_c \Delta u^2$ , which is the free-diffusion time over the distance  $(u_{\text{max}} - u_0)$ , or the natural time of re-folding of the force-free open state.

We must mention several factors that would make the process of auto-inhibition more complicated, and its rate  $K_-$  deviate from the simple expression (8). First of all, the  $[o]$  state will in most cases be quickly phosphorylated, which means there will be an additional binding energy  $\Delta G_a$  stabilising this conformation – making the effective rate of autoinhibition much lower. On the other hand, there is an effect of extension-elasticity of talin (36, 37) that would provide an additional returning force acting on the FAK complex: this would make the low/zero force case fold back faster, at a higher rate  $K_-$ . While these are interesting and important questions that need to be investigated, at the moment we will focus on the simplest approximation to understand the universal qualitative features of FAK sensor dynamics.

In order to be able to compare different expressions, and plot different versions of transition rates, we must identify the non-dimensional scaling of  $K_-$ . Factoring the same natural time scale as we used for  $K_+$ , the expression takes the form:

$$K_- = \left( \frac{\Delta G_o}{u_0^2 \gamma_c} \right) \frac{g \bar{f}^2}{(e^{g \bar{f} \lambda} - 1) - g \bar{f} \lambda}, \quad (9)$$

where, as before: the force is scaled as  $f = \bar{f} \Delta G_o / u_0$ , the opening energy barrier  $g = \Delta G_o / k_B T$ , and the ratio of two length scales (in  $[c]$  and  $[o]$  states) is labelled by the parameter  $\lambda = (u_{\text{max}} - u_0) / u_0$  (see Fig. 1). We don't have direct structural information about the physical extent of FAK opening. However, taking the structural data on the separate FAK domains from the work of Eck, Schaller and Guan (23, 39, 40), we make an estimate that  $u_{\text{max}} \approx 6.5$  nm, essentially determined by the double of the size of folded kinase domain, cf. Fig. 1. This gives  $\lambda \approx 6$  and lets us plot the comparison of the two transition rates,  $\bar{K}_+$  and  $\bar{K}_-$ .

Figure 9 gives the transition rates,  $K_+(f, \kappa)$  and  $\bar{K}_-(f)$ , plotted as a function of increasing pulling force. The rate of closing,  $\bar{K}_-$ , does not depend on the substrate parameters

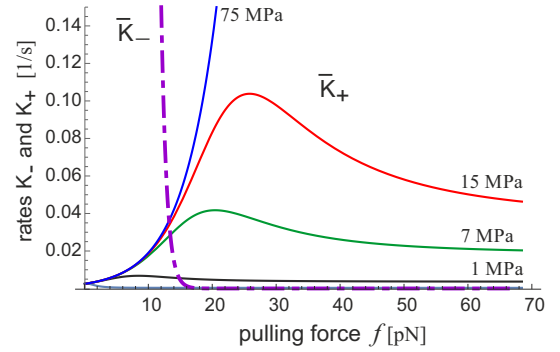


Figure 9: Comparison of the opening and closing rates,  $K_+$  and  $K_-$ , for several different substrate stiffnesses. As in several previous plots,  $\Delta G_o = 25k_B T$ ,  $u_0 = 0.9$  nm, and the damping constant ratio  $\zeta = 10^{-8}$ . When the cytoskeleton pulling force is too low, the rate of autoinhibition rapidly increases and one does not expect strong phosphorylation and positive feedback of mechanosensor.

and is rapidly increasing when the  $[c]$ - $[o]$  range of protein potential energy is flat, cf. Fig. 2. In this range of parameters, the product  $g \bar{f} \lambda$  in the equation (9) is large, and the expression decays exponentially:  $\exp[-g \bar{f} \lambda]$ . This implies that the transition from the strongly autoinhibited population of FAK sensors to the largely activated sensors is rather sharp. We find that the crossover force at which  $K_+ \approx K_-$  is a relatively universal prediction, giving an estimate for the order of magnitude force required to keep the FAK conformation open as  $f^* \approx 15$  pN.

One might be tempted, in the traditional way, to interpret the ratio of the 'on' and 'off' rates  $K_+/K_-$  as an equilibrium concentration of closed and open/activated states. However, we must remember that this process of mechanosensing is inherently non-equilibrium, even though it might be steady-state on the time scale of sensor response. Even in the regime of very low pulling forces, when  $K_- \gg K_+$ , the few FAK

molecules that are spontaneously open would provide the required (low) level of signal to the cell pathways. It is simply an indication of sensor reversibility: Fig. 9 predicts that as soon as the force reduces below  $f^*$ , most of the FAK molecules would fold back and autoinhibit their action.

## 7 Conclusions

Figures 5 and 6 each contain lots of information, but when we link the two we uncover the true nature of this reversible mechanosensor. If we place a cell on a substrate of given stiffness  $\kappa_f$  (or Young modulus  $Y_f$ ), then according to our model, the cell will increase tension in the cytoskeleton to a homeostatic level  $f(\kappa_f)$ , identified with the position of the peaks in Fig. 5. If we look at the sensitivity of the FAK complex at this fixed level of force,  $f(\kappa_f)$ , we find the maximum of sensitivity (identified with the peaks in Fig. 6b) is nothing but the actual substrate stiffness,  $\kappa_f$ . So, this model describes an adaptive sensor: not only does cytoskeletal tension adjust according to the substrate stiffness, but this remodelling adapts the sensor response so that it remains most sensitive to its immediate surroundings – small changes in the substrate stiffness will give large changes in the activation rate of FAK.

This is desirable behaviour in a biological sensor, and it is remarkable that it is produced in our model with no prior stipulation. We initially only required that the cell be responsive to changes in the stiffness – how big these changes were, or if they were optimal, was not close to the front of our minds. For such a simple model to go on and predict useful adaptive sensing behaviour is exciting to us.

Our model of a single focal adhesion kinase is obviously not the whole story. There have been several experimental works showing that FAK dimerisation is an important initiator of FAK autophosphorylation. We did not attempt to capture any collective effects in the present model, and acknowledge that there is significant ground to be gained in expanding our model to a one describing the allosteric coupling. Nevertheless, one can easily see how such collective effects might be generated within our model.

Phosphorylated FAK acts on several important signalling molecules, such as Rho and Rac. If these molecules act to increase the tension in actin filaments in the broad vicinity, rather than strictly for filaments attached to active FAK molecules, then it is obvious that there will be a cooperative effect – once a single focal adhesion kinase autophosphorylates, the tension in surrounding filaments will increase, and this increases the probability of a second opening event, and so on. This sort of collective behaviour might be effectively described using an Ising model of coupled on-off states.

The dependence of the FAK opening rate on stress relaxation partly explains results obtained in experimental work on cell spreading with different viscoelastic substrates (48).

Chaudhuri et al. saw suppression of cell spreading (associated with lower FAK activation) on substrates with significant stress relaxation, compared with purely elastic substrates of nominally the same storage modulus. We should note that we fail to capture the behaviour Chaudhuri et al. observed at very low stiffness (1.4kPa). On such a soft substrate, they saw that the number of cells with stress fibers was actually enhanced on substrates with stress relaxation – the opposite trend to stiffer substrates. This isn't surprising; our model deals with mature focal adhesion complexes. It is entirely possible that mechanosensing mechanisms other than FAK take prevalence on extremely soft substrates (and in planktonic suspension): after all, the very name of FAK suggests its relation to focal adhesions, which only occur on stiff substrates. Examining Fig. 5(a), we again wish to highlight that cells on really stiff substrates do not like to develop any additional tension (there is no positive maximum in the rate). This idea corresponds very well with experimental work showing that cells on sufficiently soft substrates do not form stable focal adhesions (56).

In summary, this work develops a theoretical model of physical mechanism a reversible mechanosensor of the 2nd kind should use. We focus all our discussion on the focal adhesion kinase, in association with integrin and talin, connecting the force-providing cytoskeletal F-actin and the varying-stiffness ECM. However, the fundamental principles of the model apply to all reversible molecular complexes that may be represented by the two-spring model of Fig. 3. The next steps are to link the main result of this work (the rate of opening  $K_+$ ) with the non-linear dynamics of one or several signaling pathways that produce the morphological response of the cell to the signal generated by mechanosensor.

### *Author contribution*

All authors contributed to carrying out research and writing the paper.

### *Acknowledgments*

We have benefited from many useful discussions and support of G. Fraser, K. Chalut, T. Alliston, X. Hu, and D. C. W. Foo. This work has been funded by EPSRC EP/M508007/1.

## References

1. Provenzano, P. P., D. R. Inman, K. W. Eliceiri, and P. J. Keely, 2009. Matrix density-induced mechanoregulation of breast cell phenotype, signaling and gene expression through a FAK–ERK linkage. *Oncogene* 28:4326–4343.
2. Barcus, C. E., P. J. Keely, K. W. Eliceiri, and L. A. Schuler, 2013. Stiff collagen matrices increase tumorigenic prolactin signaling in breast cancer cells. *J. Biol. Chem.* 288:12722–12732.

3. Bershadsky, A. D., M. Kozlov, and B. Geiger, 2006. Adhesion-mediated mechanosensitivity: a time to experiment, and a time to theorize. *Curr. Opin. Cell Biol.* 18:472–481.
4. Geiger, B., J. P. Spatz, and A. D. Bershadsky, 2009. Environmental sensing through focal adhesions. *Nature Rev. Mol. Cell Biol.* 10:21–33.
5. Opsahl, L. R., and W. W. Webb, 1994. Transduction of membrane tension by the ion channel alamethicin. *Biophys. J.* 66:71–74.
6. Sachs, F., 2010. Stretch-activated ion channels: what are they? *Physiology* 25:50–56.
7. Haswell, E. S., R. Phillips, and D. C. Rees, 2011. Mechanosensitive channels: what can they do and how do they do it? *Structure* 19:1356–1369.
8. Evans, E., and K. Ritchie, 1997. Dynamic strength of molecular adhesion bonds. *Biophys. J.* 72:1541–1555.
9. Bruinsma, R., 2005. Theory of force regulation by nascent adhesion sites. *Biophys. J.* 89:87–94.
10. Bell, G. I., 1978. Models for the specific adhesion of cells to cells. *Science* 200:618627.
11. Kramers, H. A., 1940. Brownian motion in the field of force. *Physica VII*:284–304.
12. Hanggi, P., 1986. Brownian motion in the field of force. *J. Stat. Phys.* 42:105–148.
13. Schwarz, U. S., T. Erdmann, and I. B. Bischofs, 2006. Focal adhesions as mechanosensors: The two-spring model. *BioSystems* 83:225–232.
14. Novikova, E. A., and C. Storm, 2013. Contractile fibers and catch-bond clusters: a biological force sensor? *Biophys. J.* 105:1336–1345.
15. Escudé, M., M. K. Rigozzi, and E. M. Terentjev, 2014. How cells feel: Stochastic model for a molecular mechanosensor. *Biophys. J.* 106:124–133.
16. Erdmann, T., and U. S. Schwarz, 2004. Stochastic dynamics of adhesion clusters under shared constant force and with rebinding. *J. Chem. Phys.* 121:8997–9017.
17. Khalil, N., 1999. TGF- $\beta$ : from latent to active. *Microbes Infect.* 1:1255–1263.
18. Tomasek, J. J., G. Gabbiani, B. Hinz, C. Chaponnier, and R. A. Brown, 2002. Myofibroblasts and mechanoregulation of connective tissue remodelling. *Nature* 4:349–363.
19. Shi, M., J. Zhu, R. Wang, X. Chen, L. Mi, T. Walz, and T. A. Springer, 2011. Latent TGF- $\beta$  structure and activation. *Nature* 474:343–349.
20. Burridge, K., K. Fath, T. Kelly, G. Nuckolls, and C. Turner, 1988. Focal adhesions: transmembrane junctions between the extracellular matrix and the cytoskeleton. *Annu. Rev. Cell Biol.* 4:487525.
21. Schaller, M. D., C. A. Borgman, B. S. Cobb, R. R. Vines, A. B. Reynolds, and J. T. Parsons, 1992. pp125-FAK, a structurally distinctive protein-tyrosine kinase associated with focal adhesions. *Proc. Natl. Acad. Sci. USA* 89:5192–5196.
22. Tilghman, R. W., J. K. Slack-Davis, N. Sergina, K. H. Martin, M. Iwanicki, E. D. Hershey, H. E. Beggs, L. F. Reichardt, and J. T. Parsons, 2005. Focal adhesion kinase is required for the spatial organization of the leading edge in migrating cells. *J. Cell Sci.* 118:2613–2623.
23. Lietha, D., X. Cai, D. F. J. Ceccarelli, Y. Li, M. D. Schaller, and M. J. Eck, 2007. Structural basis for the autoinhibition of focal adhesion kinase. *Cell* 129:1177–1187.
24. Provenzano, P. P., and P. J. Keely, 2011. Mechanical signaling through the cytoskeleton regulates cell proliferation by coordinated focal adhesion and Rho GTPase signaling. *J. Cell Sci.* 124:1195–1205.
25. K. Mitra, S., D. A. Hanson, and D. D. Schlaepfer, 2005. Focal adhesion kinase: in command and control of cell motility. *Nature Rev. Mol. Cell Biol.* 6:56–68.
26. Yang, B., Z. Z. Lieu, H. Wolfenson, F. M. Hameed, A. D. Bershadsky, and M. P. Sheetz, 2016. Mechanosensing controlled directly by tyrosine kinases. *Nano Lett.* 16:5951–5961.
27. Zaidel-Bar, R., C. Ballestrem, Z. Kam, and B. Geiger, 2003. Early molecular events in the assembly of matrix adhesions at the leading edge of migrating cells. *J. Cell. Sci.* 116:4605–4613.
28. Hynes, R. O., 1992. Integrins: versatility, modulation, and signaling in cell adhesion. *Cell* 69:11–25.
29. Hynes, R. O., 2002. Integrins: bidirectional, allosteric signaling machines. *Cell* 110:673–687.
30. Giancotti, F. G., 2000. Complexity and specificity of integrin signalling. *Nature Cell Biol.* 2:E14.
31. Guan, J.-L., J. E. Trevithick, and R. O. Hynes, 1991. Fibronectin/integrin interaction induces tyrosine phosphorylation of a 120-kDa protein. *Cell Reg.* 2:951–964.
32. Guan, J.-L., and D. Shalloway, 1992. Fibronectin/integrin interaction induces tyrosine phosphorylation of a 120-kDa protein. *Nature* 358:690–692.
33. Dunty, J. M., V. Gabarra-Niecko, M. L. King, D. F. J. Ceccarelli, M. J. Eck, and M. D. Schaller, 2004. FERM domain interaction promotes FAK signaling. *Mol. Cell Biol.* 24:5353–5368.
34. Schlaepfer, D. D., M. A. Broome, and T. Hunter, 1997. Fibronectin-stimulated signaling from a focal adhesion kinase-Src complex: involvement of the Grb2, p130cas, and Nck adaptor proteins. *Mol. Cell Biol.* 17:1702–1713.
35. Hytönen, V. P., and B. Wehrle-Haller, 2016. Mechanosensing in cell-matrix adhesions - Converting tension into chemical signals. *Exp. Cell Res.* 343:35–41.
36. Margadant, F., L. L. Chew, X. Hu, H. Yu, N. Bate, X. Zhang, and M. P. Sheetz, 2011. Mechanotransduction in vivo by repeated talin stretch-relaxation events depends upon vinculin. *PLoS Biol.* 9:e1001223.
37. Yao, M., B. T. Goult, B. Klapholz, X. Hu, C. P. Toseland, Y. Guo, P. Cong, M. P. Sheetz, and J. Yan, 2016. The mechanical response of talin. *Nature Comm.* 7:11966.
38. Zhou, J., C. Aponte-Santamaria, S. Sturm, J. T. Bullerjahn, A. Bronowska, and F. Gräter, 2015. Mechanism of focal adhesion kinase mechanosensing. *PLoS Comp. Biol.* 11:e1004593.
39. Cai, X., D. Lietha, D. F. Ceccarelli, A. V. Karginov, Z. Rajfur, K. Jacobson, K. M. Hahn, M. J. Eck, and M. D. Schaller, 2008. Spatial and temporal regulation of focal adhesion kinase activity in living cells. *Mol. Cell Biol.* 28:201214.
40. Zhao, J., and J.-L. Guan, 2009. Signal transduction by focal adhesion kinase in cancer. *Cancer Metastasis Rev.* 28:35–49.
41. Schlaepfer, D. D., S. K. Mitra, and D. Ilic, 2004. Control of motile and invasive cell phenotypes by focal adhesion kinase. *Biochem. Biophys. Acta* 1692:77–102.
42. Kalgin, I. V., A. Caffisch, S. F. Chekmarev, and M. Karplus, 2013. New insights into the folding of a miniprotein in a

- reduced space of collective hydrogen bond variables. *J. Phys. Chem. B* 117:6092–6105.
43. Brinkman, H. C., 1956. Brownian motion in a field of force. II. *Physica XXII*:149–155.
  44. Dudko, O. K., G. Hummer, and A. Szabo, 2006. Intrinsic rates and activation free energies from single-molecule pulling experiments. *Phys. Rev. Lett.* 96:108101.
  45. Langer, J. S., 1969. Statistical theory of the decay of metastable states. *Ann. Phys. (N.Y.)* 54:258–275.
  46. Yohichi, S., and O. K. Dudko, 2009. Single-molecule rupture dynamics on multidimensional landscapes. *Phys. Rev. Lett.* 104:048101.
  47. Gardiner, C. W., 1985. *Handbook of Stochastic Methods*. Springer-Verlag, Berlin, 2 edition.
  48. Chaudhuri, O., L. Gu, M. Darnell, D. Klumpers, S. A. Bencherif, J. C. Weaver, N. Huebsch, and D. J. Mooney, 2015. Substrate stress relaxation regulates cell spreading. *Nature Comm.* 6:6364.
  49. Buscemi, L., D. Ramonet, F. Klingberg, A. Formey, J. Smith-Clerc, J.-J. Meister, and B. Hinz, 2011. The single-molecule mechanics of the latent TGF- $\beta$ 1 Complex. *Curr. Biol.* 21:2046–2054.
  50. Brenner, M. D., R. Zhou, and H. T., 2011. Forcing a connection: impacts of single-molecule force spectroscopy on in vivo tension sensing. *Biopolymers* 95:332344.
  51. Lecuit, T., P. F. Lenne, and E. Munro, 2011. Force generation, transmission, and integration during cell and tissue morphogenesis. *Annu. Rev. Cell Dev. Biol.* 27:157184.
  52. Landau, L. D., and I. M. Lifshitz, 1986. *Theory of Elasticity*. Butterworth-Heinemann, Oxford, 3 edition.
  53. Böhmer, R., H. Senapati, and C. A. Angell, 1991. Mechanical stress relaxation in inorganic glasses studied by a step-strain technique. *J. Non-Cryst. Sol.* 131-133:182–186.
  54. Smith, G. D., and D. Bedrov, 2007. Relationship between the  $\alpha$ - and  $\beta$ -relaxation processes in amorphous polymers. *J. Polym. Sci. B* 45:627–643.
  55. Crane, R. M., and J. W. Gillespie, 1991. Characterization of the vibration damping loss factor of glass. *Comp. Sci. Tech.* 40:355–375.
  56. Trappmann, B., J. E. Gautrot, J. T. Connelly, D. G. T. Strange, Y. Li, M. L. Oyen, M. A. C. Stuart, H. Boehm, B. Li, V. Vogel, J. P. Spatz, F. M. Watt, and W. T. S. Huck, 2012. Extracellular-matrix tethering regulates stem-cell fate. *Nat. Mater.* 11:642–649.